

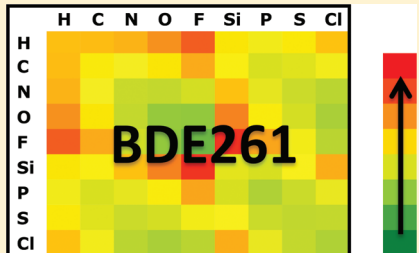
BDE261: A Comprehensive Set of High-Level Theoretical Bond Dissociation Enthalpies

Bun Chan* and Leo Radom*

School of Chemistry and ARC Centre of Excellence for Free Radical Chemistry and Biotechnology, University of Sydney, Sydney, NSW 2006, Australia

 Supporting Information

ABSTRACT: We have used the high-level W1w protocol to compile a comprehensive collection of 261 bond dissociation enthalpies (BDEs) for bonds connecting hydrogen, first-row and second-row p-block elements. Together they cover 45 bond types, and we term this the BDE261 set. We have used these benchmark values to assess the performance of computationally less demanding theoretical procedures, including density functional theory (DFT), double-hybrid DFT (DHDFT), and high-level composite procedures. We find that the M06-2X (DFT), ROB2-PLYP and DuT-D3 (DHDFT), and G3X(MP2)-RAD and G4(MP2)-6X (composite) procedures yield absolute BDEs with satisfactory to excellent accuracy. Overall, we recommend G4(MP2)-6X as an accurate and relatively cost-effective procedure for the direct computation of BDEs. One important finding is that the deviations for DFT and (especially) DHDFT procedures are often quite systematic. This allows an alternative approach to obtaining accurate *absolute* BDEs, namely, to evaluate accurate *relative* BDEs (RBDEs) using a computationally less demanding procedure, and to use these RBDEs in combination with appropriate and accurate reference BDEs to give accurate absolute BDEs. We recommend DuT-D3 for this purpose. For a still less computationally demanding approach, we introduce the *deviation from additivity of the RBDE* (DARBDE), and demonstrate that the combination of lower-level DARBDEs for larger systems and higher-level (W1w) reference RBDEs and BDEs for small systems can be utilized to obtain improved RBDEs for multiply substituted systems at low cost.



INTRODUCTION

The strength of a chemical bond is central to chemistry. It determines the energy of a reaction where existing bonds are broken and new bonds are formed, which is often a critical feature that influences chemical reactivity.¹ Therefore, the knowledge of accurate bond dissociation enthalpies (BDEs) is of fundamental importance. While many BDEs have been determined experimentally,² computational quantum chemistry has in recent years emerged to be an increasingly viable alternative for the accurate evaluation of bond strengths and thermochemical properties more generally.³

The application of highly accurate computational chemistry procedures, typically involving coupled-cluster with single, double, and perturbative triple excitations [CCSD(T)] at the complete-basis-set (CBS) limit, however, remains prohibitive for all but the smallest molecules. Therefore, theoretical procedures that are both adequately accurate but less demanding on computational resources are crucial to the further advancement of the theoretical evaluation of BDEs. In this regard, methods such as the G_n composite protocols⁴ and density functional theory (DFT) procedures⁵ are potentially attractive. However, these less expensive methodologies are often associated with somewhat larger uncertainties, and it is unclear if a procedure that is accurate for the evaluation of one thermochemical property is equally adequate for other thermochemical properties.

To develop confidence in the quality of theoretically calculated quantities, critical evaluation of the performance of computational procedures is essential. For BDEs, there have been numerous benchmark studies on theoretical methods.⁶ For example, a number of DFT and composite procedures have been benchmarked for their ability to reproduce high-level theoretical C–H BDEs.^{6b,i} Likewise, the performance of various methods for the determination of O–H BDEs^{6g} and N–H BDEs^{6j} has been assessed. Xu and co-workers have examined a number of DFT procedures for the calculation of BDEs for a number of bond types.^{6f,h} There has also been an investigation of the performance of DFT procedures for the calculation of BDEs in radical reactions.^{6c}

These studies have provided useful insights into the appropriate theoretical procedures for the calculation of specific BDEs. Notwithstanding this, it would be desirable to systematically survey the performance of a variety of computational methods for a wider range of BDEs, in an attempt to provide a general set of recommendations. In the present study, we have investigated the BDEs for substrates of the form $X_i(H_j)Y-ZH_k$, where Y and Z are hydrogen, first-row or second-row p-block elements (C, N, O, F, Si, P, S, or Cl), and

Received: March 16, 2012

Revised: April 26, 2012

Published: May 15, 2012

Table 1. BDE261 Set of W1w Bond Dissociation Enthalpies (298 K, kJ mol^{-1})

	H	CH_3	NH_2	OH	F	SiH_3	PH_2	SH	Cl
H	436.1	439.0	450.3	498.0	571.9	385.3	345.3	381.2	432.2
Me_3C	405.9	365.6	360.6	402.8	489.1	333.9	279.5	305.3	357.3
Me_2HC	412.8	369.7	361.0	399.7	483.1	342.3	284.9	308.0	357.0
MeH_2C	424.0	373.3	357.9	394.0	474.3	355.2	291.2	308.8	354.7
H_3C	439.0	377.9	354.6	385.6	462.9	372.4	300.4	311.7	350.7
FH_2C	424.2	389.5	403.0	432.8	501.7	343.1	286.2	317.4	355.6
F_2HC	426.8	407.7	410.3	458.9	534.7	335.3	287.9	313.5	361.1
F_3C	448.4	432.4	438.9	481.4	547.4	358.0	304.2	323.6	363.3
Me_2N	394.9	331.1	254.0	260.1	297.6	381.5	263.7	244.1	239.6
MeHN	418.5	341.6	271.3	264.5	295.7	405.1	297.7	263.1	248.3
H_2N	450.3	354.6	276.1	266.7	291.7	432.9	321.3	279.4	256.1
FHN	381.6	321.6	287.5	264.4	276.6	348.4	249.0	234.9	211.0
F_2N	313.4	276.0	235.8	223.3	245.3	265.8	177.0	155.7	150.1
MeO	440.7	351.3	232.5	183.3	187.2	468.2	327.3	256.0	202.9
HO	498.0	385.6	266.7	208.0	201.9	520.0	376.1	293.2	233.4
FO	419.5	349.7	281.3	195.0	165.5	435.7	306.0	263.7	179.4
F	571.9	462.9	291.7	201.9	155.0	636.7	468.3	347.0	254.9
Me_3Si	396.5	389.5	459.7	553.8	677.8	329.0	317.2	398.1	497.0
Me_2HSi	393.1	384.8	454.0	545.8	667.0	326.3	311.9	390.2	486.5
MeH_2Si	389.1	378.8	444.1	534.9	653.1	323.5	305.5	379.8	473.3
H_3Si	385.3	372.4	432.9	520.0	636.7	321.1	299.1	368.8	458.2
FH_2Si	396.2	395.9	477.7	563.2	675.9	324.3	311.7	393.9	484.4
F_2HSi	406.7	413.4	494.1	585.9	695.2	330.2	322.4	401.8	496.1
F_3Si	424.1	432.3	506.3	591.5	697.1	349.3	335.3	409.2	498.0
Me_2P	336.3	310.7	343.7	409.8	506.6	287.2	244.3	294.1	356.9
MeHP	340.1	305.4	334.2	394.4	488.6	292.7	242.0	287.4	343.0
H_2P	345.3	300.4	321.3	376.1	468.3	299.1	240.5	278.0	327.0
FHP	330.3	311.0	371.7	426.0	514.9	271.7	236.4	297.5	348.1
F_2P	316.9	317.4	387.8	458.6	557.6	241.3	224.2	289.6	363.6
MeS	364.2	307.9	284.4	303.3	363.3	353.8	268.1	268.1	276.7
HS	381.2	311.7	279.4	293.2	347.0	368.8	278.0	266.1	267.7
FS	351.7	315.6	338.9	338.2	379.7	336.7	266.5	287.2	277.4
Cl	432.2	350.7	256.1	233.4	254.9	458.2	327.0	267.7	239.5

X is either a methyl or a fluoro substituent (see Table 1 below). This yields 45 bond types and a total of 261 unique BDEs, which also cover the effect of prototypical σ -substituents on the BDEs. We will refer to this set as BDE261. We have obtained BDEs for the BDE261 set with the high-level W1w procedure,^{7,8} which provides an excellent estimate of relativistic all-electron complete-basis-set CCSD(T) energies, and have used these benchmark values to assess the performance of a representative set of DFT and composite methods.

COMPUTATIONAL DETAILS

Standard ab initio molecular orbital theory and DFT calculations^{5,9} were carried out with the Gaussian 09,¹⁰ Molpro 2010,¹¹ MRCC,¹² and ORCA¹³ programs. Geometries were optimized with the B3-LYP/cc-pVTZ+d procedure, which is the prescribed method in the W1w protocol. Following each geometry optimization, harmonic frequency analysis was carried out to confirm the nature of the stationary point as an equilibrium structure. Our benchmark energies were

obtained with the W1w composite procedure,^{7,8} which employs a series of CCSD and CCSD(T) calculations to approximate the all-electron relativistic CCSD(T)/CBS level. In a number of cases showing significant deviations from experimental BDEs, we have examined the importance of post-CCSD(T) correlation effects, and the use of larger basis sets for the CBS extrapolation. We find that they are small ($\leq 2.7 \text{ kJ mol}^{-1}$) for the systems examined.

Literature values⁴ for corrections for spin-orbit coupling, where available, were included for selected open-shell species.¹⁴ To obtain the zero-point vibrational energies (ZPVEs) and thermal corrections for enthalpies at 298 K (ΔH_{298}), we used B3-LYP/cc-pVTZ+d harmonic vibrational frequencies. In accord with the W1w protocol, a scale factor of 0.985 was applied to the calculated harmonic frequencies. All relative enthalpies correspond to 298 K values in kJ mol^{-1} .

In the present study, we have investigated the performance of a variety of DFT and composite methods. While there are a large number of DFT procedures from which to choose, we

note that many popular functionals can be loosely grouped into a relatively small number of categories. First, there is the now ubiquitous B3-LYP¹⁵ and related functionals. The second class contains procedures that are based on the PBE¹⁶ functional form, while the third class is related to the B97¹⁷ procedure. Thus, we have examined the hybrid functionals B3-LYP, PBE1-PBE,¹⁸ and B98,¹⁹ the related range-separated²⁰ forms CAM-B3-LYP,²¹ LC- ω PBE,²² and ω B97X,²³ and the dispersion-corrected²⁴ variants B3-LYP-D3,²⁴ PBE1-PBE-D3,²⁴ and B98-D3.²⁵ Furthermore, we have investigated B3-P86,¹⁵ which has previously been found to perform well for N-X (X = H, Cl) BDEs,^{6j} as well as M06-2X,²⁶ which has been shown to yield accurate results for a wide variety of thermochemical properties.^{26,27} The 6-311+G(3df,2p) basis set was used in conjunction with all the DFT procedures.

For the dispersion corrections, we have examined the use of the original zero-damping variant [D3(0)],²⁴ as well as the Becke-Johnson variant [D3(BJ)].²⁸ We find that the use of D3(BJ) generally leads to absolute values for BDEs that are in closer agreement with W1w, but the D3(0) variant usually yields smaller deviations for relative BDEs. Values presented in the text and denoted D3 correspond to D3(0) quantities. This choice is based on the better performance of D3(0) for the relative BDEs which, as we shall see, is where the strength of DFT procedures lies. The D3(BJ) results are included in the Supporting Information, Tables S7–S9.

We have examined a number of double-hybrid DFT (DHDFT) procedures, namely, B2-PLYP,²⁹ PoT,³⁰ and DuT.³⁰ The first of these is Grimme's original double-hybrid functional, while the latter two are among the latest DHDFT procedures. The PoT and DuT methods make use of separate scaling of the opposite- and same-spin components of the MP2 correlation energy,³¹ and they are optimized to be used with specific triple- ζ -type basis sets. We have also investigated the dispersion-corrected variants B2-PLYP-D3,³² PoT-D3³⁰, and DuT-D3,³⁰ and in addition the ROB2-PLYP³³ procedure, which has been found to perform well for the evaluation of C–H BDEs.⁶ⁱ For B2-PLYP, B2-PLYP-D3, and ROB2-PLYP, all electrons were correlated in the MP2 treatment, and the aug- $\text{def}2\text{-QZVP}$ basis set, which employs $\text{def}2\text{-QZVP}$ augmented with diffuse functions from the aug-cc-pVQZ basis set for non-hydrogen atoms, was used. For PoT, DuT, PoT-D3, and DuT-D3, the chemical core was frozen in the evaluation of the MP2 correlation energy. For PoT and PoT-D3, the 6-311+G(3df,2p)+d basis set³⁰ was used, while the aug-cc-pVTZ+d basis set³⁰ was employed for DuT and DuT-D3.

We use the term DFT in the text to refer to conventional methods that do not contain an MP2 component, while double-hybrid DFT procedures are referred to generally as DHDFT. The DFT and DHDFT procedures mentioned above represent a small selection of illustrative examples of the different classes of DFT-type methods, and the results obtained with these methods will be discussed in detail in the text. In addition to these procedures, we have also examined the performance of a number of other DFT and DHDFT methods. These include the DFT procedures B3-PW91,³⁴ B3-PW91-D3,²⁷ M06-2X-D3,²⁷ PW6-B95-D3,³² CAM-B3-LYP-D3,²⁷ and LC- ω PBE-D3,²⁷ and the DHDFT methods PWP-B95-D3³² and DSD-PBE-P86.³⁵ The results obtained with these procedures are given in the Supporting Information, Tables S7–S9.

For composite protocols, we have examined a number of $G_n(\text{MP2})$ -type methods including $G4(\text{MP2})$ ³⁶ and two of its

variants, namely, $G4(\text{MP2})\text{-5H}$ ³⁷ and $G4(\text{MP2})\text{-6X}$,³⁸ and also $G3X(\text{MP2})\text{-RAD}$,³⁹ which has been found to perform well for the calculation of C–H BDEs.⁶ⁱ In addition, we have investigated the higher-level methods $G4^c$ and CBS-QB3.⁴⁰ For the sake of consistency, in the case of these composite procedures, the B3-LYP/cc-pVTZ+d structures and scaled vibrational frequencies were used instead of the prescribed geometries.

We use the benchmark W1w results to assess the performance of the computationally less demanding procedures. Statistical quantities examined include mean absolute deviations (MADs), mean deviations (MDs), largest deviations (LDs), and number of outliers with deviations of more than $i \text{ kJ mol}^{-1}$ (NO_i), all taken relative to the W1w values.

RESULTS AND DISCUSSION

Accuracy Considerations. The W1w BDE261 set is intended to be a collection of wide-ranging high-accuracy theoretical BDEs. It is therefore appropriate to first address the question: what is the accuracy to be expected for these BDEs? The W1w protocol has been found to provide an excellent approximation to the CCSD(T) energy at the CBS limit.⁷ Therefore, one can reasonably expect that the key shortcomings of W1w would largely be associated with the shortcomings of the CCSD(T) method itself, notably the truncation of the electron correlation effect at the "(T)" perturbative triples level. To this end, it has been proposed that the importance of "post-(T)" effects, that is, correlation effects that are not covered by CCSD(T), can be assessed from the percentage of the energy contribution of the (T) term to the total atomization energy (TAE).⁴¹ We will abbreviate this diagnostic tool as %[(T)].

It has been suggested⁴¹ that post-(T) effects are *qualitatively* mild for %[(T)] < 4%. Higher excitation effects are somewhat more important for %[(T)] between 4 and 10%, and become fairly significant for %[(T)] beyond 10%. We have briefly reanalyzed the data given in the Supporting Information of reference 41b, and have formed a complementary set of propositions for assessing the importance of post-(T) contribution to *energy*. Thus, we propose that, for %[(T)] < 4%, it is quite likely that the post-(T) contribution to TAE (abbreviated as $E[(T)+]$) is <2 kJ mol⁻¹. For %[(T)] < 7%, one may reasonably find $E[(T)+]$ to be <4 kJ mol⁻¹. Beyond 7%, it becomes more probable to have (significantly) larger $E[(T)+]$ values (>4 kJ mol⁻¹).

Using these guidelines, we find that, for the 294 species employed in the BDE261 set, 266 species are likely to have $E[(T)+]$ < 2 kJ mol⁻¹. For the remaining 28 species, one may reasonably expect $E[(T)+]$ < 4 kJ mol⁻¹ in 17 cases, while there may be larger uncertainties for 11 species. Out of these 11 cases, literature $E[(T)+]$ values are available for five species.^{41b} We find that the $E[(T)+]$ values in these five cases are all <4 kJ mol⁻¹, with the largest being 3.72 kJ mol⁻¹ for FOF, which has a %[(T)] of 14.8%. For the remaining six species that have %[(T)] > 7%, most do not exceed this cutoff value by a large amount (%[(T)] ~ 7–9%), with only FOCI having a substantially larger %[(T)] of 13.1%. In this case, we have estimated an approximate $E[(T)+]$ value of 2.1 kJ mol⁻¹.⁴²

It is also noteworthy that post-(T) correlation effects, in general, lead to larger TAEs.^{41b} The systematic nature of the sign of $E[(T)+]$ allows for some cancellation of errors for relative quantities such as BDEs. Taking all of the above into account, we can be reasonably confident that virtually all of the

BDEs in the BDE261 set are “chemically accurate”, with a maximum uncertainty of $\sim 4\text{--}5 \text{ kJ mol}^{-1}$.

General Observations for the BDEs. The BDE261 set of W1w BDEs are shown in Table 1. It is important to keep in mind that the BDEs depend on the enthalpies of both the product fragments and the precursor molecule. Put more loosely, the BDEs depend on the “stabilities” of the radicals relative to those of the parent molecules. The stabilities of radicals is a topic of continuing investigation, and qualitative guidelines regarding the effect of substituents have been presented.^{61,43} For example, for carbon-centered radicals, the stability is generally enhanced by electron-donating substituents and with π -delocalization, but it is diminished with electron-withdrawing substituents.

There are also a number of effects that influence the stabilities of the precursor molecules. One of these is that a difference in the electronegativities of the fragments leads to ionic character that strengthens the bond.⁴⁴ Indeed, Mó et al., in a study of a large set of BDEs,⁴⁵ found that the BDEs increase as the electronegativity difference between the fragments widens. In the present study, we also observe the largest BDEs for the highly polar Si–F bonds (Table 1).

We have briefly examined the atomic charges in the molecules, obtained with natural population analysis (NPA) at the B3-LYP/6-311+G(3df,2p) level (Supporting Information, Table S3).⁴⁶ We find that, for Si–F bonds, the BDEs generally parallel the differences in the charges (Q) on the Si and F atoms: $\text{H}_3\text{Si–F}$ (BDE = $636.7 \text{ kJ mol}^{-1}$, $\Delta Q = 1.923$) < $\text{MeH}_2\text{Si–F}$ ($653.1, 2.150$) < $\text{Me}_2\text{HSi–F}$ ($666.5, 2.375$) < $\text{FH}_2\text{Si–F}$ ($675.9, 2.445$) \sim $\text{Me}_3\text{Si–F}$ ($677.3, 2.569$) < $\text{F}_2\text{HSi–F}$ ($694.7, 2.854$) \sim $\text{F}_3\text{Si–F}$ ($696.6, 3.195$). For less polar bonds, we find that the correlation is often less good, as other effects appear to become relatively more important.

Comparison with Experiment. For 112 molecules in the BDE261 set, the corresponding experimental BDEs are available from reference 2 (Supporting Information, Table S4). A comparison between the W1w and experimental values shows that in 77 of these cases, the differences between the theoretical and experimental values are less than 5 kJ mol^{-1} ; in 23 cases, the differences lie between 5 and 10 kJ mol^{-1} ; and in 12 cases, the differences exceed 10 kJ mol^{-1} , with some discrepancies as large as 120 kJ mol^{-1} ! Ten of the molecules showing discrepancies greater than 10 kJ mol^{-1} are sufficiently small in size that we were able to further refine our calculated BDEs at the higher W1w+T(Q)^{6g} and W2w⁷ levels. The W1w +T(Q) procedure differs from W1w in that post-CCSD(T) correlation is included at the CCSDT(Q) level, while W2w utilizes larger basis sets for the extrapolation to the CBS limit when compared with W1w.

A comparison between the W1w, W1w+T(Q), W2w, and experimental values is shown in Table 2. It can be seen that the W1w, W1w+T(Q), and W2w values agree well with one another in all cases. Thus, it appears that higher excitations and larger basis sets for the CBS extrapolation do not significantly alter these calculated BDEs. Given that the large discrepancies between experiment and the high-level theoretical values remain, we recommend re-evaluation of the experimental BDEs in all these cases.

We note that, in the particular cases of the BDEs for FS–H, HS–F, and FS–Cl, where the experimental values are all lower than the theoretical BDEs by $\sim 115 \text{ kJ mol}^{-1}$, the compendium values² were all derived from information reported in a kinetic study⁴⁷ of gas-phase ion reactions. The quantities used in the

Table 2. Comparison of W1w, W1w+T(Q), W2w and Experimental BDEs (298 K, kJ mol^{-1}) for Selected Molecules in the BDE261 Set Where There Are Significant Discrepancies Between Theory and Experiment

	W1w	W1w+T(Q)	W2w	expt
FHN–F	276.6	277.8	275.6	294.6
F ₂ N–Cl	150.1	150.5	151.5	134.0
MeO–SH	256.0	256.7	257.0	234.0
H ₃ Si–PH ₂	299.1	299.4	299.8	331.4
MeHP–H	340.1	340.1	339.7	322.2
H ₂ P–PH ₂	240.5	241.1	242.0	256.1
FS–H	351.7	351.4	351.5	237.9
HS–F	347.0	348.5	346.8	229.5
MeS–Cl	276.7	277.5	279.1	292.9
FS–Cl	277.4	278.3	280.1	162.3

derivation² were heats of formation (ΔH_f 's) for FSH (-7 kJ mol^{-1}) and FSCl (-28 kJ mol^{-1}). However, these values were reported in the original experimental paper as *upper-bound* values rather than actual ΔH_f 's.⁴⁷ Thus, the BDEs for FS–H, HS–F, and FS–Cl given in reference 2 are in fact *lower bounds* to these BDEs, and in this sense are all consistent with our theoretical values, albeit being poor approximations to them. At the W1w level, the ΔH_f value for HS• ($140.3 \text{ kJ mol}^{-1}$) is in good agreement with the experimental value⁴⁸ ($139.33 \text{ kJ mol}^{-1}$). For FS•, the W1w value (6.1 kJ mol^{-1}) lies somewhat further from the experimental value ($12.97 \text{ kJ mol}^{-1}$). On the other hand, we have obtained ΔH_f values of -124.8 and $-148.6 \text{ kJ mol}^{-1}$ for FSH and FSCl, respectively, which are substantially more negative than the reported upper-bound values of -7 and -28 kJ mol^{-1} , respectively. This would account for the large discrepancy between theory and experiment for the BDEs in these three cases.

Performance of DFT Procedures for BDEs. We now examine the performance of the various less demanding procedures for the evaluation of the BDEs (Table 3). Among the hybrid DFTs, namely, B3-LYP, PBE1-PBE, B98, B3-P86, and M06-2X, B3-LYP gives the largest mean absolute deviation (MAD) of 26.7 kJ mol^{-1} . In addition, it also produces a value for the largest deviation (LD) with the greatest magnitude, as well as yielding the largest number of outliers (NO). The PBE1-PBE, B98, and B3-P86 procedures give progressively smaller MADs of $18.0, 15.0$, and 11.6 kJ mol^{-1} , respectively, while M06-2X performs the best with an MAD of just 6.5 kJ mol^{-1} . We find that the large deviations for B3-LYP, and to a smaller extent, for PBE1-PBE, B98, and B3-P86, are primarily associated with a systematic underestimation of the BDEs. This is evident from the large and negative mean deviations (MDs), as well as standard deviations (SDs) that are not significantly larger than that for the best performing M06-2X method.

The range-separated DFT procedures CAM-B3-LYP (MAD = 18.9 kJ mol^{-1}) and ω B97X (MAD = 8.4 kJ mol^{-1}) give improved performance when compared with the hybrid DFTs on which they are based, namely, B3-LYP (MAD = 26.7 kJ mol^{-1}) and B98 (15.0 kJ mol^{-1}), respectively. However, the MAD for LC- ω PBE (19.5 kJ mol^{-1}) is slightly larger than that for PBE1-PBE (18.0 kJ mol^{-1}). We note that the deviations for the range-separated DFTs are again mainly associated with the systematic underestimation of BDEs, as indicated by the negative MD values that are comparable in magnitude to the MADs. We also see that the SDs for the range-separated DFTs are somewhat smaller than those for the corresponding hybrids,

Table 3. Statistical Performance^a (kJ mol⁻¹) of DFT, Double-Hybrid DFT (DHDFT), and Composite Procedures against Benchmark W1w BDEs

	MAD	MD	LD	SD	NO ₅	NO ₁₀	NO ₂₀
DFT							
B3-LYP	26.7	-26.7	-51.9	9.7	260	245	196
PBE1-PBE	18.0	-18.0	-45.5	8.8	250	214	98
B98	15.0	-14.9	-35.8	7.0	243	200	51
B3-P86	11.6	-10.3	-37.1	9.7	192	136	45
M06-2X	6.5	-5.0	-23.4	6.9	124	65	9
Range-Separated DFT							
CAM-B3-LYP	18.9	-18.9	-39.3	7.5	251	220	124
LC- ω PBE	19.5	-19.5	-39.1	6.5	254	233	136
ω B97X	8.4	-8.1	-25.9	5.5	187	86	7
Dispersion-Corrected DFT							
B3-LYP-D3	22.2	-22.2	-38.8	7.5	259	240	180
PBE1-PBE-D3	15.3	-15.3	-41.7	8.3	242	194	62
B98-D3	7.3	-7.1	-27.2	5.7	158	67	10
DHDFT							
B2-PLYP	12.6	-12.6	-24.8	4.3	254	185	6
PoT	8.8	-8.7	-20.7	3.3	225	94	1
DuT	7.3	-7.2	-13.9	2.7	205	43	0
ROB2-PLYP	4.4	-4.2	-14.5	3.4	103	11	0
Dispersion-Corrected DHDFT							
B2-PLYP-D3	10.2	-10.1	-17.6	3.2	249	138	0
PoT-D3	8.0	-8.0	-20.7	3.2	215	67	1
DuT-D3	6.4	-6.4	-13.1	2.5	178	19	0
Composite Procedures							
G4(MP2)	5.9	-5.7	-15.4	3.5	147	32	0
G4(MP2)-5H	5.4	-5.2	-12.1	3.3	138	17	0
G4(MP2)-6X	4.8	-4.7	-11.4	2.8	124	7	0
G3X(MP2)-RAD	4.4	-4.2	-14.5	3.4	103	11	0
G4	3.6	-3.6	-7.9	1.6	45	0	0
CBS-QB3	2.2	1.6	7.2	2.3	22	0	0

^aMAD = mean absolute deviation, MD = mean deviation, LD = largest deviation, SD = standard deviation, NO_i = number of outliers where the deviation is larger than *i* kJ mol⁻¹.

indicating that the deviations are becoming somewhat more systematic.

As expected from the underestimation of BDEs by the B3-LYP, PBE1-PBE, and B98 procedures, the use of a dispersion correction generally leads to smaller MADs. However, there is still substantial under-binding by the B3-LYP-D3 and PBE1-PBE-D3 procedures, with MD values of -22.2 and -15.3 kJ mol⁻¹, respectively. For B98, the inclusion of the D3 correction gives an MAD of 7.3 kJ mol⁻¹, which is comparable to that for M06-2X (6.5 kJ mol⁻¹). We note that the dispersion-corrected procedures also have somewhat smaller SDs when compared with the corresponding methods without the D3 term. We further note that the inclusion of dispersion corrections for range-separated DFT procedures also leads to better agreement with the W1w benchmark (Supporting Information, Tables S7–S9). However, for M06-2X, the BDEs obtained with the dispersion-corrected variant, that is, M06-2X-D3, are very similar to those for M06-2X itself.⁴⁹

Performance of DFT Procedures for Relative BDEs. As all the DFT procedures examined display systematic underestimation of the *absolute* BDEs, one can envisage that they would yield better performance for *relative* BDEs, which should benefit from the cancellation of systematic deviations. We have

investigated six schemes for obtaining relative BDEs, with increasing level of sophistication:

- (1) RBDE1a: All BDEs are measured relative to the H–H BDE.
- (2) RBDE1b: All BDEs are measured relative to the H₃C–H BDE.
- (3) RBDE1c: All BDEs are measured relative to the H₃C–CH₃ BDE.
- (4) RBDE3: This scheme combines the features of RBDE1a, b and c. The BDE of H–H is measured relative to H₂ itself, and therefore always has a zero RBDE by definition. The BDE of a bond involving a heavy atom and a hydrogen atom is measured relative to that of H₃C–H, while those for bonds between two heavy atoms are measured relative to the H₃C–CH₃ BDE. Thus, this scheme involves three reference BDEs.
- (5) RBDE5: This is a slightly refined scheme when compared with RBDE3. H₂ has a zero RBDE by definition. RBDEs of bonds between a heavy atom and a hydrogen are measured relative to the H₃C–H BDE, bonds between two first-row atoms employ the H₃C–CH₃ BDE as reference, BDEs for bonds between a first-row and a second-row atom are measured relative to that for H₃C–SiH₃, and BDEs that involve two second-row atoms are measured relative to the H₃Si–SiH₃ BDE. A total of five reference BDEs are used in this scheme.⁵⁰
- (6) RBDE45: Every bond type employs its own reference BDE, which is the corresponding unsubstituted system. For example, the bonds Me₂HC–NH₂ and Me₂N–CH₃ use the H₃C–NH₂ BDE as the reference, and the reference for F₂N–H is the H₂N–H BDE. The BDE261 set contains 45 bond types and hence this relative BDE scheme involves 45 reference BDEs.

The MADs for the various types of RBDEs obtained by the different theoretical procedures are shown in Table 4. In general, the MADs for the RBDEs are smaller than those for BDEs (Table 3), and become progressively smaller with increasing sophistication of the RBDE scheme, with the smallest MADs generally found for RBDE45. For DFT procedures, M06-2X achieves the smallest MAD of just 2.0 kJ mol⁻¹ for RBDE45. For the three simplest RBDE protocols, namely, RBDE1a, RBDE1b, and RBDE1c, the use of the H–H BDE as the reference in RBDE1a and the H₃C–H BDE in RBDE1b yields substantially larger MADs for the B3-based procedures (B3-LYP, B3-P86, CAM-B3LYP, and B3-LYP-D3) than those for other DFTs. This is probably associated with the uncharacteristically close agreement of the CH₃–H and (especially) H–H BDEs with the W1w values for the B3-based methods, leading to a decreased benefit from cancellation of errors.

As the BDE261 set is dominated by bonds between heavy atoms, one might have expected the use of H₃C–CH₃ in the RBDE1c scheme to be a better choice than H–H or H₃C–H. What we actually observe is a better performance for RBDE1c when compared with RBDE1a and RBDE1b for some functionals (e.g., B3-type procedures), but a somewhat less good performance for other procedures (e.g., PBE-based procedures, ω B97X and B98-D3).

Overall, M06-2X continues to be among the best performing DFT procedures, with relatively consistent MADs for the different RBDE protocols, and the smallest MAD of all the DFT procedures when the most sophisticated RBDE45 scheme

Table 4. MADs (kJ mol⁻¹) for the Various Procedures for the Calculation of Relative BDEs Using Different Schemes^{a,b}

	RBDE1a	RBDE1b	RBDE1c	RBDE3	RBDE5	RBDE45
DFT						
B3-LYP	29.6	20.1	8.2	7.4	6.6	6.1
PBE1-PBE	7.6	7.6	10.1	9.5	7.4	5.1
B98	6.5	9.8	8.7	8.8	7.3	6.7
B3-P86	20.6	15.0	8.5	8.6	7.3	6.0
M06-2X	5.8	5.7	6.9	6.4	6.9	2.0
Range-Separated DFT						
CAM-B3-LYP	17.2	14.0	7.0	6.8	5.4	4.7
LC- ω PBE	5.2	6.1	7.5	7.2	5.1	4.8
ω B97X	6.3	5.8	10.6	9.8	9.6	5.0
Dispersion-Corrected DFT						
B3-LYP-D3	25.1	15.8	6.4	5.7	4.9	4.2
PBE1-PBE-D3	8.8	6.3	9.5	8.7	6.7	3.9
B98-D3	5.5	4.3	8.9	8.1	5.5	3.9
DHDFT						
B2-PLYP	9.3	7.4	3.5	3.4	3.2	3.5
PoT	6.6	6.4	3.2	3.3	2.2	1.4
DuT	4.2	5.3	2.8	2.9	1.8	1.6
ROB2-PLYP	2.8	3.7	3.1	3.2	2.9	2.8
Dispersion-Corrected DHDFT						
B2-PLYP-D3	6.8	5.1	2.6	2.5	2.4	2.4
PoT-D3	5.9	5.7	3.1	3.1	2.1	1.1
DuT-D3	3.4	4.5	2.6	2.7	1.7	1.3
Composite Procedures						
G4(MP2)	10.1	4.9	3.5	3.6	3.2	2.3
G4(MP2)-5H	9.6	3.4	2.8	2.6	3.4	1.3
G4(MP2)-6X	11.0	3.6	2.3	2.3	2.3	1.2
G3X(MP2)-RAD	10.6	3.0	2.7	2.3	2.4	2.0
G4	5.2	2.3	1.8	1.8	1.8	1.0
CBS-QB3	3.2	1.8	1.8	1.8	2.6	1.0

^aMADs calculated relative to W1w values. ^bRBDE1a uses H–H as the reference BDE, H₃C–H is used for RBDE1b, H₃C–CH₃ for RBDE1c, H–H, H₃C–H and H₃C–CH₃ for RBDE3, H–H, H₃C–H, H₃C–CH₃, H₃C–SiH₃ and H₃Si–SiH₃ for RBDE5, and all 45 unsubstituted systems for RBDE45, see text for a more detailed description.

is employed. We find that many DFT procedures, notably the dispersion-corrected methods, give small overall MADs for RBDEs using the RBDE45 scheme. However, it has been demonstrated that some DFT procedures exhibit difficulty for the evaluation of substituent effects,⁵¹ and we introduce an approach below to overcome such situations. For the moment, we note that we also observe difficulty in describing substituent effects, to differing extents, for nearly all of the functionals for most bond types examined (for an example, see Supporting Information, Table S5). In this connection, we find that the M06-2X procedure is the most successful of the DFT procedures in estimating substituent effects.

We note that, although the RBDE45 scheme involves more reference calculations than other RBDE protocols, it does produce the quantitatively most accurate results. This is particularly true when it is used together with a relatively robust DFT method such as M06-2X. The use of the combination of RBDE45 and M06-2X is especially attractive when only a small number of bond types are involved.

Performance of DHDFT and Composite Procedures.

We now turn our attention to the double-hybrid DFT and composite procedures. For the evaluation of absolute BDEs (Table 3), DHDFT procedures perform from adequately to favorably, with B2-PLYP giving the largest MAD of 12.6 kJ mol⁻¹, while the smallest MADs are seen for ROB2-PLYP (4.4 kJ mol⁻¹) and DuT-D3 (6.4 kJ mol⁻¹). We note that the

ROB2-PLYP BDEs are obtained with a quadruple- ζ basis set and with correlation of all electrons, while DuT-D3 utilizes a triple- ζ basis set and the frozen-core approximation, and so is computationally less demanding.

The deviations for the DHDFT procedures are largely systematic, as evident from the MD values that are comparable in magnitude to the MADs, and as also reflected in the small SDs of \sim 2–4 kJ mol⁻¹. When the systematic deviations are minimized using an appropriate relative BDE scheme such as RBDE3, RBDE5, or RBDE45 (Table 4), the MADs are \leq 3.5 kJ mol⁻¹. The smallest MADs of \sim 1–1.5 kJ mol⁻¹ are achieved by the PoT, DuT, PoT-D3, and DuT-D3 procedures using the RBDE45 scheme. When the less complicated RBDE5 protocol is utilized, DuT and DuT-D3 somewhat outperform the other DHDFT procedures, with an MAD of <2 kJ mol⁻¹, versus \sim 2–3 kJ mol⁻¹ for the rest of the DHDFT methods under this RBDE scheme. We note that small MADs for absolute BDEs are also observed for the DHDFT procedures PWP-B95-D3 (4.9 kJ mol⁻¹ with the aug'-def2-TZVP basis set) and DSD-PBE-P86 (3.7 kJ mol⁻¹ with the aug'-def2-QZVP basis set) (Supporting Information, Table S7). However, these methods show relatively large SD values (5.0 and 3.3 kJ mol⁻¹, for PWP-B95-D3 and DSD-PBE-P86, respectively), which are indicative of somewhat larger nonsystematic deviations. This leads to comparatively poorer performance for RBDEs for these two procedures [MADs of 5.8 and 2.5 kJ mol⁻¹, respectively, for

Table 5. MADs (kJ mol⁻¹) for BDEs Calculated for the Different Bond Types in the BDE261 Set for M06-2X, DuT-D3 and G4(MP2)-6X^a

	H	C	N	O	F	Si	P	S	Cl
M06-2X									
H	5.6	6.1	4.7	8.3	11.7	14.6	6.3	6.1	5.4
C	6.1	1.8	3.0	3.9	1.7	10.7	2.6	2.5	1.5
N	4.7	3.0	5.2	4.1	1.3	6.2	1.8	2.0	2.7
O	8.3	3.9	4.1	4.5	11.1	10.9	2.7	4.7	2.5
F	11.7	1.7	1.3	11.1	23.4	18.9	8.7	5.4	2.2
Si	14.6	10.7	6.2	10.9	18.9	22.3	13.9	12.4	9.9
P	6.3	2.6	1.8	2.7	8.7	13.9	5.0	3.3	1.6
S	6.1	2.5	2.0	4.7	5.4	12.4	3.3	2.0	0.4
Cl	5.4	1.5	2.7	2.5	2.2	9.9	1.6	0.4	1.0
DuT-D3									
H	3.2	3.0	3.3	4.2	6.8	3.5	4.2	5.2	6.0
C	3.0	5.4	4.9	4.4	4.6	6.6	6.8	7.1	7.6
N	3.3	4.9	4.5	4.9	5.1	5.4	5.4	5.8	7.8
O	4.2	4.4	4.9	5.6	6.8	5.4	4.8	5.2	6.9
F	6.8	4.6	5.1	6.8	12.7	7.5	6.6	6.6	8.8
Si	3.5	6.6	5.4	5.4	7.5	8.5	8.9	9.6	10.4
P	4.2	6.8	5.4	4.8	6.6	8.9	8.8	8.8	9.5
S	5.2	7.1	5.8	5.2	6.6	9.6	8.8	9.5	10.4
Cl	6.0	7.6	7.8	6.9	8.8	10.4	9.5	10.4	11.9
G4(MP2)-6X									
H	6.3	2.2	4.1	4.6	0.4	4.1	2.2	3.4	1.6
C	2.2	3.9	4.6	5.4	2.7	6.4	3.3	3.1	1.9
N	4.1	4.6	5.6	5.0	1.7	8.4	5.5	4.7	1.8
O	4.6	5.4	5.0	5.5	1.6	9.2	5.5	5.6	2.4
F	0.4	2.7	1.7	1.6	3.4	5.1	1.5	1.6	2.0
Si	4.1	6.4	8.4	9.2	5.1	8.9	7.1	7.5	6.2
P	2.2	3.3	5.5	5.5	1.5	7.1	4.5	4.9	3.0
S	3.4	3.1	4.7	5.6	1.6	7.5	4.9	5.2	2.5
Cl	1.6	1.9	1.8	2.4	2.0	6.2	3.0	2.5	1.0

^aMADs calculated relative to W1w values.

values obtained with the RBDE5 scheme (Supporting Information, Table S8), and 3.5 and 1.4 kJ mol⁻¹, respectively, for RBDE45 (Supporting Information, Table S9)] when compared with DuT-D3.

The composite procedures, in general, perform somewhat better than the DHDFT methods for the evaluation of absolute BDEs (Table 3). The *Gn*(MP2)-type procedures give MADs of ~4–6 kJ mol⁻¹, with G3X(MP2)-RAD (4.4 kJ mol⁻¹) performing the best, followed by G4(MP2)-6X (4.8 kJ mol⁻¹). The G4(MP2), G4(MP2)-5H, and G4(MP2)-6X methods employ the same single-point-energy components and therefore bear the same computational cost. They differ only in the manner of manipulating and combining the constituent energies. Thus, among these three procedures, it appears advantageous to employ G4(MP2)-6X for the evaluation of BDEs since it produces the smallest MADs. The more expensive and rigorous G4 and CBS-QB3 procedures yield still smaller MADs of 3.6 and 2.2 kJ mol⁻¹, respectively, when compared with the *Gn*(MP2)-type procedures.

The deviations for the composite procedures appear to be mildly systematic, as indicated by the comparable magnitudes for the MADs and the corresponding MDs. However, the magnitudes of systematic deviations are already quite small (MD ~ 4–6 kJ mol⁻¹ for *Gn*(MP2)-type procedures and 2–4 kJ mol⁻¹ for G4 and CBS-QB3), and are comparable to the magnitudes for the nonsystematic deviations (SD ~ 3 kJ mol⁻¹

for *Gn*(MP2)-type procedures and ~2 kJ mol⁻¹ for G4 and CBS-QB3). Therefore, we do not expect substantial improvement in performance for the evaluation of relative BDEs. Indeed, the composite procedures generally perform only comparably to the DHDFT procedures for relative BDEs (Table 4). We note that the various *Gn*(MP2)-type procedures give notably less accurate results than DHDFT methods when the RBDE1a scheme is employed.⁵² In general, for the evaluation of relative BDEs, the less expensive DHDFT procedures such as DuT-D3 appear to be more cost-effective.

Performance for Specific Bond Types. In this section, we examine the performance of M06-2X, DuT-D3, and G4(MP2)-6X as representative DFT, DHDFT, and composite procedures in the calculation of BDEs of specific bond types. The cost for these three procedures increases in the order: M06-2X < DuT-D3 < G4(MP2)-6X, with relative timing of 1.0 (M06-2X), 3.0 (DuT-D3), and 6.1 (G4(MP2)-6X) for the total CPU times required for the calculation of the complete BDE261 set.

Table 5 shows the MADs from W1w values for the absolute BDEs of the 45 bond types for M06-2X, DuT-D3, and G4(MP2)-6X, while Table 6 lists the MADs for the corresponding RBDEs. We first point out that the number of entries for the various bond types are different from one bond type to another. For instance, there is only one possibility for each of the following bond types: H–H, F–H, Cl–H, F–F,

Table 6. MADs (kJ mol⁻¹) for RBDEs Calculated for the Different Bond Types in the BDE261 Set for M06-2X, DuT-D3 and G4(MP2)-6X^a

	H	C	N	O	F	Si	P	S	Cl
M06-2X (RBDES)									
H	0.0	3.0	1.7	5.3	8.7	11.6	3.3	3.1	2.4
C	3.0	2.4	2.3	3.1	1.2	1.3	6.8	7.5	10.9
N	1.7	2.3	4.4	3.5	1.1	3.2	11.0	11.4	12.0
O	5.3	3.1	3.5	5.3	12.0	1.7	6.7	8.1	7.9
F	8.7	1.2	1.1	12.0	24.2	9.5	1.4	4.0	7.2
Si	11.6	1.3	3.2	1.7	9.5	0.7	7.7	9.1	11.6
P	3.3	6.8	11.0	6.7	1.4	7.7	16.5	18.6	20.4
S	3.1	7.5	11.4	8.1	4.0	9.1	18.6	19.5	21.7
Cl	2.4	10.9	12.0	7.9	7.2	11.6	20.4	21.7	22.6
M06-2X (RBDE45)									
H	0.0	3.0	0.9	0.7	0.0	1.1	0.9	0.9	0.0
C	3.0	2.4	3.0	3.0	2.9	1.3	2.1	2.8	2.3
N	0.9	3.0	3.7	4.5	2.0	1.4	1.9	2.1	2.3
O	0.7	3.0	4.5	2.8	2.0	1.3	2.7	5.1	3.0
F	0.0	2.9	2.0	2.0	0.0	1.3	2.5	1.1	0.0
Si	1.1	1.3	1.4	1.3	1.3	0.7	1.5	1.8	1.7
P	0.9	2.1	1.9	2.7	2.5	1.5	1.1	2.1	2.3
S	0.9	2.8	2.1	5.1	1.1	1.8	2.1	0.7	0.6
Cl	0.0	2.3	2.3	3.0	0.0	1.7	2.3	0.6	0.0
DuT-D3 (RBDES)									
H	0.0	1.0	1.4	2.2	4.9	1.6	2.2	3.2	4.0
C	1.0	1.1	1.1	1.7	2.0	1.5	1.5	1.8	2.4
N	1.4	1.1	1.3	2.0	1.4	1.7	1.1	0.7	2.5
O	2.2	1.7	2.0	1.3	2.5	2.1	1.9	1.2	1.6
F	4.9	2.0	1.4	2.5	8.4	2.5	1.9	1.4	3.5
Si	1.6	1.5	1.7	2.1	2.5	0.7	1.2	1.9	2.7
P	2.2	1.5	1.1	1.9	1.9	1.2	1.0	1.1	1.7
S	3.2	1.8	0.7	1.2	1.4	1.9	1.1	1.7	2.7
Cl	4.0	2.4	2.5	1.6	3.5	2.7	1.7	2.7	4.1
G4(MP2)-6X (RBDES)									
H	0.0	0.9	2.7	3.3	1.8	2.8	0.8	2.1	0.2
C	0.9	2.0	1.9	1.8	1.9	1.7	2.8	3.0	4.2
N	2.7	1.9	2.2	1.3	2.1	2.5	1.2	1.8	4.2
O	3.3	1.8	1.3	1.7	2.3	3.2	0.7	1.1	3.6
F	1.8	1.9	2.1	2.3	7.2	0.9	4.5	4.4	8.0
Si	2.8	1.7	2.5	3.2	0.9	1.5	1.4	1.1	1.5
P	0.8	2.8	1.2	0.7	4.5	1.4	3.2	2.8	4.7
S	2.1	3.0	1.8	1.1	4.4	1.1	2.8	2.5	5.2
Cl	0.2	4.2	4.2	3.6	8.0	1.5	4.7	5.2	8.7

^aMADs calculated relative to W1w values.

Cl, and Cl–Cl. At the other end of the spectrum, there are 13 C–Si bonds in the BDE261 set.

For absolute BDEs (Table 5), we can see that M06-2X gives MADs that lie below 5 kJ mol⁻¹ for many bond types. Notable exceptions are some BDE types that involve H, F, and (particularly) Si. To assess whether basis set deficiency might be causing the larger deviations found for bonds that involve these elements, we have carried out additional M06-2X BDE calculations using the larger aug-cc-pV(Q+d)Z basis set (Supporting Information, Table S6). This includes diffuse functions and a larger and balanced set of polarization functions for all elements, and additional tight-d functions for second-row p-block elements. We find that, while the overall performance is somewhat improved, bonds that involve H, F, and Si still lead to less good agreement with benchmark W1w values. Thus, it appears that the modest difficulty in the evaluation of these

BDEs lies within the M06-2X functional itself, but the exact cause is not yet clear.⁵³

In comparison with M06-2X, DuT-D3 seems to produce a relatively more consistent performance across most bond types, with F–F, Si–Cl, S–Cl, and Cl–Cl being the only bond types with MADs that are larger than 10 kJ mol⁻¹. For many types of bonds, the MADs are between 3–6 kJ mol⁻¹. However, bonds that include F or Cl, and BDEs that involve two second-row elements appear to lead to somewhat larger MADs.

For G4(MP2)-6X, the MADs are smaller than ~5 kJ mol⁻¹ for most bond types, with bonds that involve O and (particularly) Si being notable exceptions. We point out that, although the overall MADs for the BDE261 set decrease in the order M06-2X > DuT-D3 > G4(MP2)-6X, the performance for any particular bond type does not necessarily follow the same trend (e.g., M06-2X gives the smallest MAD for C–C bonds). Nonetheless, the good performance and better consistency of

G4(MP2)-6X make it an appealing choice for the evaluation of absolute BDEs in general.

Alternatively, owing to the systematic nature of the deviations for DuT-D3 (Table 3, Table 4 and Table 6), it may be more efficient to use this DHDFT procedure to calculate relative BDEs, for example, with the RBDE3 or RBDE5 scheme, and to use these RBDEs in conjunction with accurate W1w reference BDEs to obtain the target absolute BDEs. For instance, when DuT-D3 RBDEs (evaluated with the RBDE5 scheme) are combined with W1w BDEs, we obtain an overall MAD for the BDE261 set of just 1.7 kJ mol^{-1} for the estimated BDEs (Supporting Information, Table S2), which is already smaller than those obtained by direct calculations using G4 or CBS-QB3 (Table 3).⁵⁴

In fact, when the RBDE5 scheme is employed for the calculation of RBDEs, we find a somewhat more consistent performance across different bond types for DuT-D3 than for the higher-level G4(MP2)-6X procedure (Table 6), as well as a smaller overall MAD for all RBDEs (1.7 kJ mol^{-1} , versus 2.3 kJ mol^{-1} for G4(MP2)-6X) (Table 4). On the other hand, the combination of M06-2X and the RBDE5 scheme not only yields a relatively larger overall MAD (6.9 kJ mol^{-1} , Table 4), but also shows a somewhat inconsistent performance for different bond types (Table 6). Therefore, we again emphasize that, when one uses M06-2X for the evaluation of RBDEs, it is advantageous to use the RBDE45 scheme.

DARBDEs and the Application to the Evaluation of RBDEs and BDEs. As mentioned above, some of the DFT procedures give poor relative BDEs (RBDEs). In this section, we define the *deviation from additivity of the RBDE* (DARBDE), and demonstrate that it may be obtained to significantly greater accuracy than the RBDE by many DFT procedures. We then proceed to show how DARBDE values may be used in conjunction with accurate reference RBDEs for small systems to give improved RBDEs and BDEs for larger systems.

To begin our discussion, we first define the *additive RBDE* (ARBDE). As an illustrative example, for substituted methanes of the form $\text{Y}_n\text{H}_{3-n}\text{C-X}$, we employ the C-X RBDE for the singly substituted system ($\text{YH}_2\text{C-X}$) as the reference for the doubly- and triply substituted substrates ($\text{Y}_2\text{HC-X}$ and $\text{Y}_3\text{C-X}$). The ARBDE is obtained as the additive effect of substitution:

$$\text{ARBDE}[\text{Y}_n\text{H}_{3-n}\text{C-X}] = n\text{RBDE}[\text{YH}_2\text{C-X}]$$

The deviation from additivity of the RBDE (DARBDE) is then simply the deviation of the actual RBDE from the ARBDE:

$$\begin{aligned} \text{DARBDE}[\text{Y}_n\text{H}_{3-n}\text{C-X}] \\ = \text{RBDE}[\text{Y}_n\text{H}_{3-n}\text{C-X}] - \text{ARBDE}[\text{Y}_n\text{H}_{3-n}\text{C-X}] \end{aligned}$$

Table 7 shows the RBDEs and DARBDEs for the series $\text{MeH}_2\text{C-OH}$, $\text{Me}_2\text{HC-OH}$, and $\text{Me}_3\text{C-OH}$ obtained by the various procedures. This series of RBDEs represents one of the difficult cases for DFT procedures encountered in reference 51. It can be seen that there is a sizable variation in the calculated RBDEs. Furthermore, while the benchmark W1w RBDEs increase in the order: $\text{MeH}_2\text{C-OH}$ (8.3 kJ mol^{-1}) < $\text{Me}_2\text{HC-OH}$ (14.0 kJ mol^{-1}) < $\text{Me}_3\text{C-OH}$ (17.1 kJ mol^{-1}), several of the DFT procedures give completely wrong trends, as noted previously.⁵¹ For example, B3-LYP gives RBDEs of 1.3 ($\text{MeH}_2\text{C-OH}$), 0.1 ($\text{Me}_2\text{HC-OH}$), and -3.8 ($\text{Me}_3\text{C-OH}$) kJ mol^{-1} . On the other hand, in contrast to the varying

Table 7. RBDEs (Relative to $\text{H}_3\text{C-OH}$) for $\text{MeH}_2\text{C-OH}$ (Et-OH), $\text{Me}_2\text{HC-OH}$ (i-Pr-OH), and $\text{Me}_3\text{C-OH}$ (t-Bu-OH), and DARBDEs for i-Pr-OH and t-Bu-OH (kJ mol^{-1})

	RBDE			DARBDE	
	Et-OH	i-Pr-OH	t-Bu-OH	i-Pr-OH	t-Bu-OH
DFT					
B3-LYP	1.3	0.1	-3.8	-2.4	-7.6
PBE1-PBE	1.9	1.7	-1.2	-2.1	-6.9
B98	0.2	-1.2	-5.0	-1.6	-5.5
B3-P86	0.8	-0.1	-3.4	-1.8	-6.0
M06-2X	5.4	9.6	12.0	-1.2	-4.2
Range-Separated DFT					
CAM-B3-LYP	3.5	4.8	3.6	-2.2	-6.9
LC- ω PBE	3.9	5.9	6.0	-1.8	-5.6
ω B97X	2.9	4.6	4.7	-1.2	-4.1
Dispersion-Corrected DFT					
B3-LYP-D3	3.7	5.9	5.6	-1.6	-5.6
PBE1-PBE-D3	3.4	5.2	4.4	-1.7	-5.9
B98-D3	3.7	7.2	9.1	-0.1	-1.9
DHDFT					
B2-PLYP	5.3	7.6	7.0	-2.9	-8.8
PoT	7.1	11.5	13.3	-2.6	-7.8
DuT	7.2	11.8	13.5	-2.7	-8.2
ROB2-PLYP	6.2	9.2	8.9	-3.2	-9.6
Dispersion-Corrected DHDFT					
B2-PLYP-D3	6.6	10.7	12.2	-2.5	-7.7
PoT-D3	7.5	12.4	14.8	-2.5	-7.5
DuT-D3	7.7	12.8	15.2	-2.5	-7.8
Composite Procedures					
G4(MP2)	7.1	11.6	13.8	-2.6	-7.6
G4(MP2)-5H	9.5	16.3	20.8	-2.6	-7.6
G4(MP2)-6X	8.5	14.4	18.0	-2.6	-7.5
G3X(MP2)-RAD	10.4	18.3	23.9	-2.5	-7.3
G4	8.1	13.8	17.0	-2.5	-7.4
CBS-QB3	8.8	15.4	19.6	-2.3	-6.8
W1w	8.3	14.0	17.1	-2.6	-7.8

performance for the RBDEs, the deviations for the DARBDEs are uniformly much smaller.

Having found that simple procedures such as DFT can give relatively accurate DARBDE values, we now demonstrate how this can be utilized, in combination with accurate reference values, to obtain improved RBDEs. As an illustrative example, we use the W1w RBDE for $\text{MeH}_2\text{C-OH}$ (8.3 kJ mol^{-1}) as our reference, and we obtain the corresponding ARBDEs for $\text{Me}_2\text{HC-OH}$ (16.6 kJ mol^{-1}) and $\text{Me}_3\text{C-OH}$ (24.9 kJ mol^{-1}). We then add the B3-LYP DARBDEs for $\text{Me}_2\text{C-OH}$ (-2.4 kJ mol^{-1}) and $\text{Me}_3\text{C-OH}$ (-7.6 kJ mol^{-1}) to the ARBDE values, and this gives estimated RBDEs of 14.2 and 17.4 kJ mol^{-1} , respectively, for $\text{Me}_2\text{HC-OH}$ and $\text{Me}_3\text{C-OH}$. These compare favorably with the W1w values of 14.0 ($\text{Me}_2\text{HC-OH}$) and 17.1 ($\text{Me}_3\text{C-OH}$) kJ mol^{-1} , and represent a massive improvement on the directly calculated B3-LYP RBDE values of 0.1 ($\text{Me}_2\text{HC-OH}$) and -3.8 ($\text{Me}_3\text{C-OH}$) kJ mol^{-1} . Furthermore, the RBDEs estimated with DARBDEs can then be combined with the W1w BDE of $\text{H}_3\text{C-OH}$ (385.6 kJ mol^{-1}) to give virtually W1w-quality BDEs for $\text{Me}_2\text{HC-OH}$ [399.9 (B3-LYP) versus 399.7 (W1w) kJ mol^{-1}] and $\text{Me}_3\text{C-OH}$ [403.0 (B3-LYP) versus 402.8 (W1w) kJ mol^{-1}].

Table 8 shows a comparison of the directly calculated RBDEs for $\text{Me}_2\text{HC-OH}$ and $\text{Me}_3\text{C-OH}$, and the RBDEs estimated using the DARBDE procedure for the various theoretical

Table 8. Directly-Calculated RBDEs (using the RBDE45 scheme) and RBDEs Estimated Using DARBDEs for $\text{Me}_2\text{HC-OH}$ (i-Pr-OH) and $\text{Me}_3\text{C-OH}$ (t-Bu-OH), and MADs for Calculated BDEs, RBDEs, and DARBDEs for the BDE261 Set (kJ mol^{-1})

	RBDE		RBDE via DARBDE		MAD		
	i-Pr	t-Bu	i-Pr	t-Bu	BDE	RBDE	DA-RBDE
DFT							
B3-LYP	0.1	-3.8	14.2	17.4	26.7	6.1	0.6
PBE1-PBE	1.7	-1.2	14.5	18.0	18.0	5.1	0.6
B98	-1.2	-5.0	15.0	19.4	15.0	6.7	0.8
B3-P86	-0.1	-3.4	14.8	18.9	11.6	6.0	0.7
M06-2X	9.6	12.0	15.4	20.7	6.5	2.0	0.7
Range-Separated DFT							
CAM-B3-LYP	4.8	3.6	14.4	18.0	18.9	4.7	0.7
LC- ω PBE	5.9	6.0	14.8	19.3	19.5	4.8	0.7
ω B97X	4.6	4.7	15.4	20.9	8.4	5.0	1.0
Dispersion-Corrected DFT							
B3-LYP-D3	5.9	5.6	15.0	19.3	22.2	4.2	0.7
PBE1-PBE-D3	5.2	4.4	14.9	19.0	15.3	3.9	0.7
B98-D3	7.2	9.1	16.5	23.0	7.3	3.9	1.0
DHDFT							
B2-PLYP	7.6	7.0	13.7	16.2	12.6	3.5	0.4
PoT	11.5	13.3	14.0	17.1	8.8	1.4	0.4
DuT	11.8	13.5	14.0	16.8	7.3	1.6	0.4
ROB2-PLYP	9.2	8.9	13.4	15.3	4.4	2.8	0.6
Dispersion-Corrected DHDFT							
B2-PLYP-D3	10.7	12.2	14.1	17.3	10.2	2.4	0.4
PoT-D3	12.4	14.8	14.1	17.4	8.0	1.1	0.4
DuT-D3	12.8	15.2	14.1	17.1	6.4	1.3	0.4
Composite Procedures							
G4(MP2)	11.6	13.8	14.0	17.3	5.9	2.3	0.3
G4(MP2)-5H	16.3	20.8	14.0	17.3	5.4	1.3	0.3
G4(MP2)-6X	14.4	18.0	14.1	17.5	4.8	1.2	0.3
G3X(MP2)-RAD	18.3	23.9	14.1	17.6	4.2	2.0	0.2
G4	13.8	17.0	14.2	17.6	3.6	1.0	0.3
CBS-QB3	15.4	19.6	14.4	18.1	2.2	1.0	0.3
W1w	14.0	17.1	14.0	17.1			

methods. The table also gives the MADs for the BDEs, the directly calculated RBDEs (obtained with the RBDE45 scheme), and the DARBDEs for the complete BDE261 set. The results discussed above for the directly calculated and DARBDE-derived RBDEs for $\text{Me}_2\text{HC-OH}$ and $\text{Me}_3\text{C-OH}$ already point toward a significant improvement for the DARBDE-based values. In general, we find that all the DFT procedures examined give DARBDE values that are in good agreement with the benchmark W1w values, as reflected in the small MAD values. Indeed, the mean absolute deviations from W1w values of the DARBDEs is $\leq 1 \text{ kJ mol}^{-1}$ throughout. These DARBDEs can then be applied to obtain improved RBDEs, and BDEs, with MADs from W1w values $\leq 1 \text{ kJ mol}^{-1}$.

CONCLUDING REMARKS

Using the high-level W1w procedure, we have calculated a set of 261 bond dissociation enthalpies that cover 45 bond types between hydrogen, first-row p-block, and second-row p-block elements. We term this the BDE261 set, and have employed it as the benchmark for the evaluation of more economical

theoretical procedures. The following key observations emerge from the present study:

- Comparison of our W1w BDEs with the experimental values listed in reference 2 generally shows very good agreement but also reveals large discrepancies in a number of cases. For the smaller systems among this group of BDEs, we have further refined our theoretical values at the W1w+T(Q) and W2w levels. These higher-level calculations yield BDEs that are consistent with W1w in all cases. We therefore recommend re-evaluation of the experimental BDEs for FHN-F , $\text{F}_2\text{N-Cl}$, MeO-SH , $\text{H}_3\text{Si-PH}_2$, MeHP-H , $\text{H}_2\text{P-PH}_2$, FS-H , HS-F , MeS-Cl , and FS-Cl .
- We have examined the performance of B3-LYP-type, PBE-type, and B97-type DFT procedures, as well as M06-2X, for the evaluation of BDEs. The M06-2X functional emerges as the overall best performer. Two procedures that are based on B97, namely, the range-separated functional ω B97X and the dispersion-corrected B98-D3 procedure, also give satisfactory performance.
- We find that the deviations for the DFT procedures are largely associated with a systematic underestimation of the BDEs. As a result, while large deviations are found for the calculated *absolute* BDEs in many of these cases, significantly improved results are often (but not always) obtained for *relative* BDEs (RBDEs). We have investigated a variety of RBDE schemes, and find that reasonably good results can be achieved with the most sophisticated RBDE45 scheme when used in combination with the M06-2X functional.
- Double-hybrid DFT (DHDFT) procedures generally give smaller overall deviations for absolute BDEs than those obtained from typical DFT procedures. Composite procedures show even better performance, as expected. We find ROB2-PLYP and DuT-D3 to be the two best-performing DHDFT procedures, while the G3X(MP2)-RAD and G4(MP2)-6X composite procedures provide more accurate absolute BDEs. For RBDEs, we find that DHDFT procedures perform as well as the composite procedures and at a lower cost.
- Regarding the performance for the BDEs of individual bond-types, we find that BDEs that involve H, F, and Si represent the more challenging cases for M06-2X. The DuT-D3 procedure offers a more uniform performance but shows some difficulty in producing accurate BDEs for bonds that involve Cl. The G4(MP2)-6X procedure provides further robustness in comparison with DuT-D3. We thus recommend G4(MP2)-6X as an accurate means for the direct calculation of absolute BDEs.
- Combination of DuT-D3 RBDEs with accurate reference BDEs provides a cost-effective alternative route to accurate absolute BDEs.
- Introduction of the *deviation from additivity of the RBDE* (DARBDE) shows that all the methods examined, including the DFT procedures that perform poorly for the evaluation of RBDEs, give quite accurate DARBDE values for all the systems in the BDE261 set. We illustrate how these relatively accurate DARBDEs can be combined with accurate reference RBDE (or BDE) values to obtain improved RBDEs (or BDEs) for multiply substituted systems, with MADs from W1w values of $\leq 1 \text{ kJ mol}^{-1}$.

■ ASSOCIATED CONTENT

■ Supporting Information

Geometries optimized at the B3-LYP/cc-pVTZ+d level in xyz format, incorporated in a single zip archive (BDE261.zip), calculated B3-LYP/cc-pVTZ+d zero-point vibrational energies (ZPVEs), enthalpy corrections at 298 K (ΔH_{298}), and W1w total electronic energies (Table S1), deviations from benchmark values (Table S2), B3-LYP/6-311+G(3df,2p) NPA charge differences for the atoms directly involved in the BDEs (Table S3), experimental BDEs from reference 2 (Table S4), deviations from W1w benchmark values for B3-LYP/6-311+G(3df,2p), M06-2X/6-311+G(3df,2p), DuT-D3, and G4-(MP2)-6X RBDEs obtained using the RBDE45 scheme (Table S5), MADs for various bond types for M06-2X/aug-cc-pV(Q+d)Z (Table S6), statistical performance of all procedures examined against benchmark W1w BDEs (Table S7), and RBDEs obtained with the RBDE5 (Table S8) and RBDE45 (Table S9) schemes. This material is available free of charge via the Internet at <http://pubs.acs.org>.

■ AUTHOR INFORMATION

Corresponding Author

*E-mail: chan_b@chem.usyd.edu.au (B.C.), radom@chem.usyd.edu.au (L.R.).

Notes

The authors declare no competing financial interest.

■ ACKNOWLEDGMENTS

We gratefully acknowledge funding (to L.R.) from the Australian Research Council (ARC) and generous grants of computer time (to L.R.) from the National Computational Infrastructure (NCI) National Facility and Intersect Australia Ltd.

■ REFERENCES

- (1) See for example: (a) Greenwood, N. N.; Earnshaw, A. *Chemistry of the Elements*, 2nd ed.; Butterworth-Heinemann: Burlington, MA, 1997. (b) Clayden, J.; Greeves, N.; Warren, S.; Wothers, P. *Organic Chemistry*; Oxford University Press: Oxford, U.K., 2001. (c) Smith, M. B.; March, J. *March's Advanced Organic Chemistry*, 5th ed.; John Wiley and Sons: New York, 2001. (d) Brown, T. L.; LeMay Jr., H. E.; Bursten, B. E.; Murphy, C. J. *Chemistry: The Central Science*, 11th ed.; Pearson Education: Upper Saddle River, NJ, 2009.
- (2) For a comprehensive compilation of experimental BDEs, see: Luo, Y.-R. *Comprehensive Handbook of Chemical Bond Energies*; CRC Press: Boca Raton, FL, 2007.
- (3) For a general overview, see: (a) Martin, J. M. L. *Ann. Rep. Comput. Chem.* **2005**, *1*, 31. (b) Fabian, W. M. F. *Monatsh. Chem.* **2008**, *139*, 309. (c) Curtiss, L. A.; Redfern, P. C.; Raghavachari, K. *WIREs Comput. Mol. Sci.* **2011**, *1*, 810. (d) Peterson, K. A.; Feller, D.; Dixon, D. A. *Theor. Chem. Acc.* **2012**, *131*, 1079.
- (4) (a) Curtiss, L. A.; Raghavachari, K.; Trucks, G. W.; Pople, J. A. *J. Chem. Phys.* **1991**, *94*, 7221. (b) Curtiss, L. A.; Raghavachari, K.; Redfern, P. C.; Rassolov, V.; Pople, J. A. *J. Chem. Phys.* **1998**, *109*, 7764. (c) Curtiss, L. A.; Redfern, P. C.; Raghavachari, K. *J. Chem. Phys.* **2007**, *126*, 084108.
- (5) For an overview on DFT see: Koch, W.; Holthausen, M. C. A. *Chemist's Guide to Density Functional Theory*, 2nd ed.; Wiley: New York, 2001.
- (6) For recent benchmark studies, see for example: (a) Fu, Y.; Liu, L.; Mou, Y.; Lin, B.-L.; Guo, Q.-X. *J. Mol. Struct.: THEOCHEM* **2004**, *674*, 241. (b) Menon, A. M.; Wood, G. P. F.; Moran, D.; Radom, L. *J. Phys. Chem. A* **2007**, *111*, 13638. (c) Izgorodina, E. I.; Brittain, D. R. B.; Hodgson, J. L.; Krenske, E. H.; Lin, C. Y.; Namazian, M.; Coote, M. L. **2007**, *111*, 10754. (d) Qi, C.; Lin, Q.-H.; Li, Y.-Y.; Pang, S.-P.; Zhang, R.-B. *J. Mol. Struct.: THEOCHEM* **2010**, *961*, 97.
- (e) Hemelsoet, K.; Van Durme, F.; Van Speybroeck, V.; Reyniers, M.-F.; Waroquier, M. *J. Phys. Chem. A* **2010**, *114*, 2864. (f) Zhang, I. Y.; Wu, J.; Luo, Y.; Xu, X. *J. Chem. Theory Comput.* **2010**, *6*, 1462.
- (g) Chan, B.; Morris, M.; Radom, L. *Aust. J. Chem.* **2011**, *64*, 394.
- (h) Zhang, I. Y.; Wu, J.; Luo, Y.; Xu, X. *J. Comput. Chem.* **2011**, *32*, 1824. (i) Menon, A. S.; Henry, D. J.; Bally, T.; Radom, L. *Org. Biomol. Chem.* **2011**, *9*, 3636. (j) O'Reilly, R. J.; Karton, A.; Radom, L. *Int. J. Quantum Chem.* **2012**, *112*, 1862.
- (7) (a) Martin, J. M. L.; De Oliveira, G. *J. Chem. Phys.* **1999**, *111*, 1843. (b) Parthiban, S.; Martin, J. M. L. *J. Chem. Phys.* **2001**, *114*, 6014. (c) Boese, A. D.; Oren, M.; Atasoylu, O.; Martin, J. M. L.; Kallay, M.; Gauss, J. *J. Chem. Phys.* **2004**, *120*, 4129.
- (8) The W1w procedure^{7c} is a slightly modified version of the W1 protocol.^{7a} It makes use of the smaller but somewhat more balanced aug'-cc-pV(n+d)Z basis sets instead of the aug'-cc-pVnZ+2d1f basis sets in the W1 procedure.
- (9) See for example: (a) Hehre, W. J.; Radom, L.; Schleyer, P. v. R.; Pople, J. A. *Ab Initio Molecular Orbital Theory*; Wiley: New York, 1986. (b) Jensen, F. *Introduction to Computational Chemistry*, 2nd ed.; Wiley: Chichester, U.K., 2007.
- (10) Frisch, M. J.; Trucks, G. W.; Schlegel, H. B.; Scuseria, G. E.; Robb, M. A.; Cheeseman, J. R.; Scalmani, G.; Barone, V.; Mennucci, B.; Petersson, G. A.; Nakatsuji, H.; Caricato, M.; Li, X.; Hratchian, H. P.; Izmaylov, A. F.; Bloino, J.; Zheng, G.; Sonnenberg, J. L.; Hada, M.; Ehara, M.; Toyota, K.; Fukuda, R.; Hasegawa, J.; Ishida, M.; Nakajima, T.; Honda, Y.; Kitao, O.; Nakai, H.; Vreven, T.; Montgomery, Jr., J. A.; Peralta, J. E.; Ogliaro, F.; Bearpark, M.; Heyd, J. J.; Brothers, E.; Kudin, K. N.; Staroverov, V. N.; Kobayashi, R.; Normand, J.; Raghavachari, K.; Rendell, A.; Burant, J. C.; Iyengar, S. S.; Tomasi, J.; Cossi, M.; Rega, N.; Millam, N. J.; Klene, M.; Knox, J. E.; Cross, J. B.; Bakken, V.; Adamo, C.; Jaramillo, J.; Gomperts, R.; Stratmann, R. E.; Yazyev, O.; Austin, A. J.; Cammi, R.; Pomelli, C.; Ochterski, J. W.; Martin, R. L.; Morokuma, K.; Zakrzewski, V. G.; Voth, G. A.; Salvador, P.; Dannenberg, J. J.; Dapprich, S.; Daniels, A. D.; Farkas, Ö.; Foresman, J. B.; Ortiz, J. V.; Cioslowski, J.; Fox, D. J. *Gaussian 09*, Revision A.02; Gaussian, Inc.: Wallingford, CT, 2009.
- (11) Werner, H.-J.; Knowles, P. J.; Manby, F. R.; Schütz, M.; Celani, P.; Knizia, G.; Korona, T.; Lindh, R.; Mitrushenkov, A.; Rauhut, G.; Adler, T. B.; Amos, R. D.; Bernhardsson, A.; Berning, A.; Cooper, D. L.; Deegan, M. J. O.; Dobbyn, A. J.; Eckert, F.; Goll, E.; Hampel, C.; Hesselmann, A.; Hetzer, G.; Hrenar, T.; Jansen, G.; Köpli, C.; Liu, Y.; Lloyd, A. W.; Mata, R. A.; May, A. J.; McNicholas, S. J.; Meyer, W.; Mura, M. E.; Nicklaß, A.; Palmieri, P.; Pflüger, K.; Pitzer, R.; Reiher, M.; Shiozaki, T.; Stoll, H.; Stone, A. J.; Tarroni, R.; Thorsteinsson, T.; Wang, M.; Wolf, A. *MOLPRO*, 2010.1; University College Cardiff Consultants Limited: Cardiff, U.K., 2010.
- (12) Källay, M.; Surján, P. R. *J. Chem. Phys.* **2001**, *115*, 2945.
- (13) Neese, F. *WIREs Comput. Mol. Sci.* **2012**, *2*, 73.
- (14) Spin-orbit corrections (millihartree) are included for OH• (-0.32), F• (-0.61), SH• (-0.86), and Cl• (-1.34).
- (15) Stephens, P. J.; Devlin, F. J.; Chabalowski, C. F.; Frisch, M. J. *J. Phys. Chem.* **1994**, *98*, 11623.
- (16) Perdew, J. P.; Burke, K.; Ernzerhof, M. *Phys. Rev. Lett.* **1996**, *77*, 3865.
- (17) Becke, A. D. *J. Chem. Phys.* **1997**, *107*, 8554.
- (18) Adamo, C.; Barone, V. *J. Chem. Phys.* **1999**, *110*, 6158.
- (19) Schmid, H. L.; Becke, A. D. *J. Chem. Phys.* **1998**, *108*, 9624.
- (20) Iikura, H.; Tsuneda, T.; Yanai, T.; Hirao, K. *J. Chem. Phys.* **2001**, *115*, 3540.
- (21) Yanai, T.; Tew, D.; Handy, N. *Chem. Phys. Lett.* **2004**, *393*, 51.
- (22) Vydrov, O. A.; Scuseria, G. E. *J. Chem. Phys.* **2006**, *125*, 234109.
- (23) Chai, J.-D.; Head-Gordon, M. *J. Chem. Phys.* **2008**, *128*, 084106.
- (24) Grimme, S.; Antony, J.; Ehrlich, S.; Krieg, H. *J. Chem. Phys.* **2010**, *132*, 154104.
- (25) The D3 correction in ref 24 for the closely related B97 functional is used.
- (26) Zhao, Y.; Truhlar, D. G. *Theor. Chem. Acc.* **2008**, *120*, 215.

- (27) Goerigk, L.; Grimme, S. *Phys. Chem. Chem. Phys.* **2011**, *13*, 6670.
- (28) (a) Becke, A. D.; Johnson, E. *J. Chem. Phys.* **2005**, *122*, 154101. (b) Grimme, S.; Ehrlich, S.; Goerigk, L. *J. Comput. Chem.* **2011**, *32*, 1456, and references therein.
- (29) Grimme, S. *J. Chem. Phys.* **2006**, *124*, 034108.
- (30) Chan, B.; Radom, L. *J. Chem. Theory Comput.* **2011**, *7*, 2852.
- (31) Kozuch, S.; Gruzman, D.; Martin, J. M. L. *J. Phys. Chem. C* **2010**, *114*, 20801.
- (32) Goerigk, L.; Grimme, S. *J. Chem. Theory Comput.* **2011**, *7*, 291.
- (33) Graham, D. C.; Menon, A. S.; Goerigk, L.; S. Grimme, S.; Radom, L. *J. Phys. Chem. A* **2009**, *113*, 9861.
- (34) Becke, A. D. *J. Chem. Phys.* **1993**, *98*, 5648.
- (35) Kozuch, S.; Martin, J. M. L. *Phys. Chem. Chem. Phys.* **2011**, *13*, 20104.
- (36) Curtiss, L. A.; Redfern, P. C.; Raghavachari, K. *J. Chem. Phys.* **2007**, *127*, 124105.
- (37) Chan, B.; Coote, M. L.; Radom, L. *J. Chem. Theory Comput.* **2010**, *6*, 2647.
- (38) Chan, B.; Deng, J.; Radom, L. *J. Chem. Theory Comput.* **2011**, *7*, 112.
- (39) Henry, D. J.; Sullivan, M. B.; Radom, L. *J. Chem. Phys.* **2003**, *118*, 4849.
- (40) (a) Montgomery, J. A., Jr.; Frisch, M. J.; Ochterski, J. W.; Petersson, G. A. *J. Chem. Phys.* **1999**, *110*, 2822. (b) Montgomery, J. A., Jr.; Frisch, M. J.; Ochterski, J. W.; Petersson, G. A. *J. Chem. Phys.* **2000**, *112*, 6532.
- (41) (a) Karton, A.; Rabinovich, E.; Martin, J. M. L.; Ruscic, B. *J. Chem. Phys.* **2006**, *125*, 144108. (b) Karton, A.; Daon, S.; Martin, J. M. L. *Chem. Phys. Lett.* **2011**, *510*, 165.
- (42) Post-(T) contributions to the energy are estimated as the sum of a CCSDT – CCSD(T) term evaluated with the cc-pVDZ and cc-pVTZ basis sets extrapolated to the CBS limit, and a CCSDT(Q) – CCSDT term obtained with cc-pVDZ.
- (43) See for example: (a) Zipse, H. *Top. Curr. Chem.* **2006**, *263*, 163. (b) De Vleeschouwer, F.; Van Speybroeck, V.; Waroquier, M.; Geerlings, P.; De Proft, F. *J. Org. Chem.* **2008**, *73*, 9109. (c) Coote, M. L.; Dickerson, A. B. *Aust. J. Chem.* **2008**, *61*, 163. (d) Coote, M. L.; Lin, C. Y.; Beckwith, A. L. J.; Zavitsas, A. A. *Phys. Chem. Chem. Phys.* **2010**, *12*, 9597. (e) Coote, M. L.; Lin, C. Y.; Zipse, H. The Stability of Carbon-Centered Radicals. In *Carbon-Centered Free Radicals and Radical Cations: Structure, Dynamics and Reactivity*; Forbes, M. D. E., Ed.; Wiley: Hoboken, NJ, 2010; pp 83–104. (f) Wodrich, M. D.; McKee, W. C.; Schleyer, P. v. R. *J. Org. Chem.* **2011**, *76*, 2439.
- (44) Pauling, L. *The Nature of the Chemical Bond*, 3rd ed.; Cornell University Press: Ithaca, NY, 1960.
- (45) Mó, O.; Yáñez, M.; Eckert-Maksić, M.; Maksić, Z. B.; Alkorta, I.; Elguero, J. *J. Phys. Chem. A* **2005**, *109*, 4359.
- (46) Reed, A. E.; Weinstock, R. B.; Weinhold, F. *J. Chem. Phys.* **1985**, *83*, 735.
- (47) Howle, C. R.; Mayhew, C. A.; Tuckett, R. P. *J. Phys. Chem. A* **2005**, *109*, 3626.
- (48) NIST Chemistry WebBook; Linstrom, P. J.; Mallard, W. G., Eds.; NIST Standard Reference Database Number 69; National Institute of Standards and Technology: Gaithersburg, MD, 2011 (<http://webbook.nist.gov>).
- (49) The D3 parametrization for M06-2X contains a zero s_8 term, which is intended to supply supplementary short-range corrections.²⁴ Because BDE261 contains relatively small molecules, the BDEs are dominated by short-range interactions, and it is not surprising that the D3 correction for M06-2X with its zero s_8 term is very small.
- (50) We have investigated the use of an additional reference BDE, namely, the $\text{H}_3\text{Si}-\text{H}$ BDE for bonds that involve a second-row atom bonded to a hydrogen atom. We find that this does not lead to significant and uniform improvements, and in fact leads to notable deterioration in performance in some cases, for example, for M06-2X RBDEs for P–H, S–H, and Cl–H bonds. We therefore do not recommend an RBDE6 scheme that adds this extra reference BDE to the RBDES scheme.
- (51) (a) Coote, M. L.; Pross, A.; Radom, L. *Org. Lett.* **2003**, *5*, 4689. (b) Coote, M. L.; Pross, A.; Radom, L. In *Fundamental World of Quantum Chemistry*; Brandas, E. J., Kryachko, E. S., Eds.; Kluwer Academic Publishers: Dordrecht, The Netherlands, 2004; Vol. III, pp 563–579. (c) Izgorodina, I.; Coote, M. L.; Radom, L. *J. Phys. Chem. A* **2005**, *109*, 7558.
- (52) We find that there are relatively large deviations for the H–H BDE for $G_n(\text{MP}2)$ -type procedures. This can be attributed to overcorrection by the higher-level-correction (HLC) in the $G_n(\text{MP}2)$ -type procedures, where the pure ab initio BDE values are already quite good. Thus, the vibrationless BDE values (kJ mol^{-1}) with no contribution from the HLC are 458.4 (W1w), 450.0 (G4), 449.0 [G4MP2)], 449.0 (G4(MP2)-SH), 458.6 (G4(MP2)-X), and 450.3 (G3X(MP2)-RAD), and the corresponding HLC contributions (kJ mol^{-1}) to the BDE are 10.0 (G4), 13.8 [G4MP2)], 13.8 (G4(MP2)-SH), 6.2 (G4(MP2)-X), and 14.7 (G3X(MP2)-RAD).
- (53) We have also examined whether the poor results are an artifact of the grid that is used, but test calculations with an ultrafine grid produce virtually identical results.
- (54) The MADs (kJ mol^{-1}) for absolute BDEs evaluated using various RBDEs and W1w reference values are 6.95 (M06-2X/RBDE5), 1.69 (DuT-D3/RBDE5), 2.28 (G4(MP2)-X/RBDE5), 2.03 (M06-2X/RBDE45), 1.34 (DuT-D3/RBDE45), and 1.15 (G4(MP2)-X/RBDE45). When the 45 reference systems in the RBDE45 scheme are excluded from the statistical analysis, the corresponding MADs are 6.61 (M06-2X/RBDE5), 1.71 (DuT-D3/RBDE5), 2.25 (G4(MP2)-X/RBDE5), 2.45 (M06-2X/RBDE45), 1.62 (DuT-D3/RBDE45), and 1.39 (G4(MP2)-X/RBDE45).